Lasers Med Sci (2014) 29:1829–1837
DOI 10.1007/s10103-014-1584-6

ORIGINAL ARTICLE

A comparison of temperature profile depending on skin types for laser hair removal therapy

Tae-Hoon Kim · Gwi-Won Lee · Jong-In Youn

Received: 18 March 2014 / Accepted: 16 April 2014 / Published online: 15 May 2014

Abstract Although numerous lasers with different wavelengths are available for laser hair removal, their use in individuals with dark-pigmented skin remains a challenge. The present study aims to develop a numerical heat diffusion model considering skin types over various wavelengths. This numerical mode uses Pennes approximation to represent heat from metabolism, blood perfusion and an external heating source. The heat diffusion model is experimentally validated by using agar-based skin tissue phantoms. Diode lasers with four different wavelengths were used with two antithetical skin models. The pulse width and beam spot size were set to 200 ms and 1 cm^2, respectively. Temperature distribution along the hair structure and skin tissue was examined to determine both thermal confinement and heat transfer to the hair follicle. Experimental results are well matched with the numerical results. The results show that for the light skin model, thermal confinement is well achieved over various wavelengths, and treatment efficacy is expected to be better at a shorter wavelength. Otherwise, for the dark skin model, thermal confinement is poorly achieved as the wavelength decreases (<808 nm) and the temperature gap between the hair tip and the hair root is significantly large compared with the light skin model, which may lead to adverse effects. We believe that the developed numerical model will help to establish optimal laser parameters for different individuals during laser hair removal.

Keywords Hair removal · Hair follicle · Heat diffusion model · Temperature distribution · Thermal confinement

T.-H. Kim · G.-W. Lee · J.-I. Youn (✉)
Department of Biomedical Engineering, College of Medical Science, Catholic University of Daegu, Gyeongsan 712-702, South Korea
e-mail: jyoun@cu.ac.kr

Introduction

Laser hair removal is a medical procedure that uses highly concentrated and pulsed light to remove hair growing on the body [1]. The main target tissue is melanin-rich hair follicles containing a population of stem cells capable of regenerating the follicle and producing hair [2]. The hair follicle can be selectively destroyed by using the appropriate wavelength, pulse duration and fluence of a light source based on the principle of selective photothermolysis [3]. During laser hair removal, two conditions should be satisfied for a successful treatment outcome: (1) delivering sufficient heat to the hair follicle to thermally destroy it and (2) achieving good thermal confinement to prevent thermal damage to non-targeted skin. To ensure these conditions, optimal laser parameters must be pre-determined based upon individual skin type before laser irradiation.

The most commonly used scheme to classify skin type according to a person's response to sun exposure in terms of burning and tanning was created in 1975 by Thomas B. Fitzpatrick [4]. The concept of skin types was first based on responses in "white" skin and later in brown skin, which was divided into three groups as follows: skin type IV for light brown, skin type V for brown skin and skin type VI for dark brown/black skin [5]. Laser hair removal is generally more effective and safer for lighter skin with dark hair than darker skin with dark hair because the epidermal melanin competes as a significant chromophore and leads to excessive heating of the surrounding tissue, which results in adverse effects such as epidermal blistering, hypopigmentation and scarring [6–9]. Type VI skin effectively absorbs as much as 40 % more energy when irradiated with visible light compared with skin types I or II when irradiated with the same fluence and pulse duration [9]. Therefore, treatment efficacy of laser hair removal is significantly reduced in persons with darker skin.

Currently used light sources for hair removal include the long-pulsed ruby (694 nm), long-pulsed alexandrite (755 nm), long-pulsed diode (810 nm), long-pulsed Nd:Yag (1,064 nm) and intense-pulsed light (590–1,200 nm) [10, 11]. The absorption coefficient of melanin decreases as wavelength increases [12]; thus, by reducing epidermal energy absorption relative to follicular absorption, longer wavelengths make it possible to treat patients with darker skin safely [13]. However, in terms of treatment efficacy, shorter wavelengths are more effective at inducing thermal effects in hair follicles owing to their higher melanin absorption [7]. In fact, the 800-nm diode laser is about 30 % less absorbed by melanin than the 694-nm ruby laser [14].

Lower treatment efficacy for darker skin types necessitates more treatment sessions than in the case of lighter skin types, which increases time and cost [15]. To reduce the associated problems of professional treatments and increase personal convenience, a handheld device has been introduced, but its relatively shorter wavelengths makes it inappropriate for darker skin types, particularly for types V and VI [6]. Alternatively, cooling devices can be used during treatment for darker skin types under physician direction. Cooling devices cool the skin either by direct contact with a cooling plate or by non-contact cooling by emitting a cooled spray of air or gas. However, the use of excessive cooling can also result in unwanted side effects such as blistering and dyspigmentation [9]. Thus, appropriate optical parameters of the light sources have to be carefully established by considering subject's skin type to achieve both thermal confinement for protection surrounding skin tissue and selective thermal destruction of hair follicles. Nevertheless, to the best of our knowledge, there has been no study to evaluate temperature profiles on skin tissue amongst different skin types using various wavelengths.

In the present study, we aimed to verify the differences of temperature distribution in multi-layered skin tissue models using a bio-heat transfer equation and suggest adequate laser wavelengths for the two antithetical skin types (type II and V) in laser hair removal. This simulation model was experimentally validated in vitro using agar-based skin tissue phantoms that included hair shafts and follicles. This model may help to determine the optimum wavelength for laser hair removal amongst different skin types, particularly for darker-skinned people.

Numerical heat diffusion (HD) simulation

The heat diffusion simulation was implemented with multiphysics using the Pennes approximation model introduced in 1948. This model has been widely used by many researchers for the analysis of bio-heat transfer phenomena [16]. It represents heat sources from tissue metabolism and blood perfusion and adds a spatial heating source in the equation, which reflects the effect of an external electromagnetic source. The equation takes the following form:

$$\rho C\frac{\partial T}{\partial t}+\nabla\cdot(-k\nabla T)=\rho_b C_b\omega_b(T_b-T)+Q_{\text{met}}+Q_{\text{ext}} \quad (1)$$

where ρ is the tissue density; C is the specific heat of tissue; k is the thermal conductivity tensor; $\rho_b C_b \omega_b$ is the source term for the blood perfusion in which ρ_b is the density of blood, C_b is the specific heat of blood and ω_b is the blood perfusion rate; T_b is the arterial blood temperature; Q_{met} is the heat source from metabolism and Q_{ext} is the external heat source term due to absorbed laser power [17]. The corresponding values are listed in Table 1. The output of the HD simulation is the dependent variable T (temperature); thus, temperature changes of the skin tissue with time can be calculated.

The heat source term is a function of both laser intensity and the Lambert–Beer law and can be written mathematically as follows:

$$Q_{\text{ext}}=Q_{\text{in}}(1-R)\alpha(\exp(-\alpha|z|)) \quad (2)$$

where Q_{in} is the incident laser power [W/m^2] at the skin surface, R is the surface reflectivity and α is the absorptivity [l/m].

The incident laser power is distributed in time and space with a Gaussian shape according to the following expression:

$$Q_{\text{in}}=Q_0\left(\frac{1}{\pi\sigma_x\sigma_y}\right)\exp\left(-\left(\frac{(x-x_0)^2}{2\sigma_x^2}+\frac{(y-y_0)^2}{2\sigma_y^2}\right)\right) \quad (3)$$

where Q_0 is the peak power of the laser beam, and the exponential term on the right-hand side represents the Gaussian distribution in the x–y plane.

By considering a cylindrical hair structure vertical to the skin surface, the skin model in this simulation is set up in a cylindrical 3D coordinate system including the epidermis, dermis, hair shaft and hair follicle, as illustrated in Fig. 1. The radius of the modelled hair is 0.1 mm, and that of the follicle is 0.3 mm. The thickness of the epidermal layer is 0.5 mm, and the dermis layer is 4 mm. For the bio-heat transfer model, except for the laser incident surface which is exposed to the ambient air at room temperature, 20 °C with a heat transfer coefficient 10 W/(m^2·K), all other domains of the tissue model remain at 37 °C.

The optical coefficients for absorption and scattering by the skin are approximated with variable amounts of melanin and blood perfusion introduced by Jacques SL [18]. Whereas the total absorption coefficient of the epidermis mainly depends on a dominant melanin absorption due to the melanosomes in

Table 1 Tissue component baseline parameters

Property	Epidermis	Dermis	Hair
Density, ρ (kg/m^3)	1,200	1,200	1,300
Thermal conductivity, k (W/(m·K))	0.21	0.53	0.37
Specific heat, C (J/(kg·K))	3,600	3,800	1,500
Blood perfusion rate, ω_b (1/s)	3e-3	3e-3	–

the epidermis, the total absorption coefficient of the dermis depends on a dominant haemoglobin absorption due to cutaneous blood perfusion. Those are calculated as below:

$$\mu_{a\_\mathrm{epi}} = (f_{\mathrm{mel}})(\mu_{a\_\mathrm{mel}}) + (1-f_{\mathrm{mel}})(\mu_{a\_\mathrm{skinbaseline}}) \quad (4)$$

$$\mu_{a\_\mathrm{derm}} = (f_{\mathrm{blood}})(\mu_{a\_\mathrm{blood}}) + (1-f_{\mathrm{blood}})(\mu_{a\_\mathrm{skinbaseline}}) \quad (5)$$

where f_{mel} is the volume fraction of melanosomes, μ_{a_mel} is the absorption coefficient of a single melanosome, f_{blood} is the average volume fraction of blood, μ_{a_blood} is the absorption coefficient of whole blood and $\mu_{a\_\mathrm{skinbaseline}}$ is the baseline absorption of both the epidermis and dermis. Skin types can be differentiated by adjusting the volume fraction of melanosomes (f_{mel}). The estimated concentration ranges from 1.3 to 43 % from light-skinned to darkly pigmented adults. In this study, we applied 3 and 22 % of the volume fraction of melanosomes to simulate skin types II (light) and V (dark), respectively, and the optical property of hair was that of black hair [19]. The total scattering coefficients were also derived from equations presented in [18]. The calculated optical properties of the tissue model over four different wavelengths are defined in Table 2.

Table 2 Optical properties of two antithetical skin models over four different wavelengths

Wavelength (nm)	660	808	860	915
Skin type	Light/dark	Light/dark	Light/dark	Light/dark
μ_{a_epi} (cm^{-1})	8.35/59.4	4.35/30.33	3.56/24.61	2.94/20.15
μ_{a_derm} (cm^{-1})	0.275/0.285	24.6/24.9	24.3/24.7	24/24.6
μ_{a_hair} (cm^{-1})	115	64	52	42
μ_{s_epi} (cm^{-1})	42/42	28/24.12	26/23.2	22/20
μ_{s_epi} (cm^{-1})	21/20	14/12.06	13/11.6	11/10

Experimental materials and methods

Phantom preparation

An experimental study was conducted to verify the HD numerical model using two-layered tissue phantoms consisting of epidermis, dermis and hair shaft with follicle. The tissue phantoms were made of agar-mixed absorber and scatterer according to the optical properties of each structure. Purified agar powder (A-7921, Sigma-Aldrich, USA) was used as a base material. Methylene blue and aluminium oxide (Al_2O_3) particles (265497, Sigma-Aldrich, USA) were used for the absorber and the scatterer, respectively. The optical properties of the methylene blue and aluminium oxide were predetermined by using an inverse adding–doubling (IAD) method from the transmittance and the reflectance measurements using integrating spheres. In order to simulate the absorption property of hair, synthetic melanin particles (M-8631, Sigma-Aldrich, USA) were added using a hypodermic needle with a 3-mm diameter which was inserted into the cured phantoms. The tissue phantoms had similar optical properties and geometry to the numerical model, except for the radius of hair shaft due to the size limitation of a hypodermic needle's diameter.

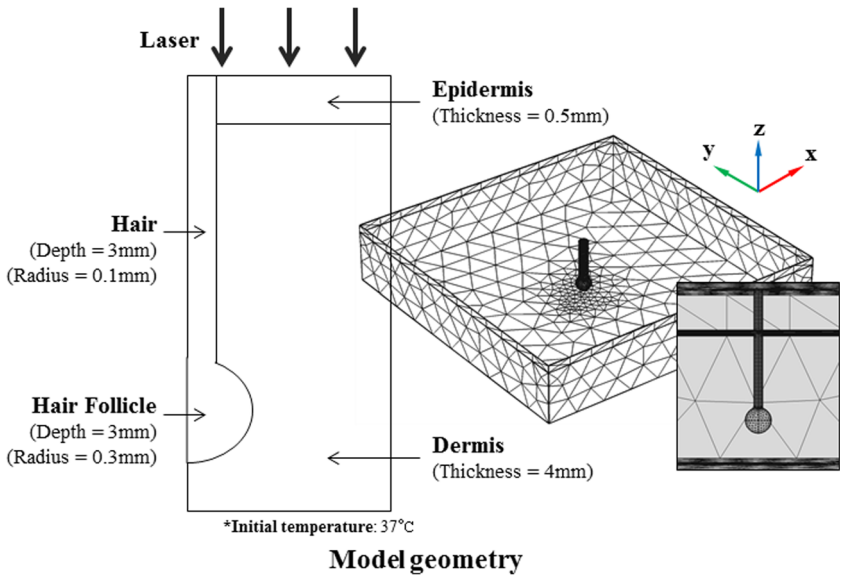

Fig. 1 Skin model geometry in a cylindrical coordinate system including epidermis, dermis, hair shaft and hair follicle

Experimental system and procedure

The experimental setup is shown in Fig. 2. The system mainly consists of two parts: (1) laser irradiation and (2) temperature measurement. In the laser irradiation part, laser diodes (LDs) with four different wavelengths (660 nm (QL65065A, QSI, Korea), 808 nm (QL80T4HD-Y, QSI, Korea), 860 nm (QL86T4HD, QSI, Korea) and 915 nm (L915P1WJ, Thorlabs, USA)) were used as heating sources. The LD was attached to a temperature-controlled mount (TCLDM9, Thorlabs, USA) and operated by an LD driver (LDC340, Thorlabs, USA). The operating currents were different according to the specifications of each laser diode, but the peak power for each was the same at 280 mW. A function generator (MXG-9810, METEX, Korea) was also used to create a square-pulse wave (pulse width, 200 ms) to the laser sources. The beam diameter on the sample surface was set to 10 mm through an aspheric condenser lens (ACL5040, Thorlabs, USA). In the temperature measurement part, a thermocouple module (TC-08, OMEGA, USA) was used to monitor real-time temperature changes in the sample. A 0.2-mm diameter thermocouple needle was inserted vertically into the sample and fixed at two pre-determined positions (hair tip and hair root). Because the two measurement points enable the needles to be superimposed during temperature recording, this measurement was performed separately for each. A total of three pulses were applied to the phantom, and the corresponding temperature increases were measured.

Results and discussion

Numerical HD model validation

An in vitro phantom experiment was conducted to validate the numerical model. Diode lasers with four different wavelengths were irradiated to the two tissue phantoms. The comparative results between the phantom experiment and the numerical simulation after three pulses are shown in Fig. 3. Laser pulse width and fluence were set to 200 ms and 71 mJ/cm^2 per pulse. In the case of the phantom experiment, since the thermocouple needle measuring the hair tip could absorb the incident light energy and lead to excessive temperature increases which are considered to be an artefact, the correction algorithm proposed by Manns et al. [20] was applied to the experimental results. We found that the two results are well matched to the two different skin models over various wavelengths. It is also found that the temperature values in the numerical model show more dynamical flow than the experimental results. One possible reason for this difference comes from different material properties between agar-based phantoms and real skin tissue, particularly from their thermodynamic properties such as density and heat capacity. Another reason may be that the elongated thermocouple needle has contact with a relatively large area in the sample, and in return, it cannot effectively measure the temperature only at the designated measuring point (hair tip), whereas point-by-point measurement is available in the numerical simulation.

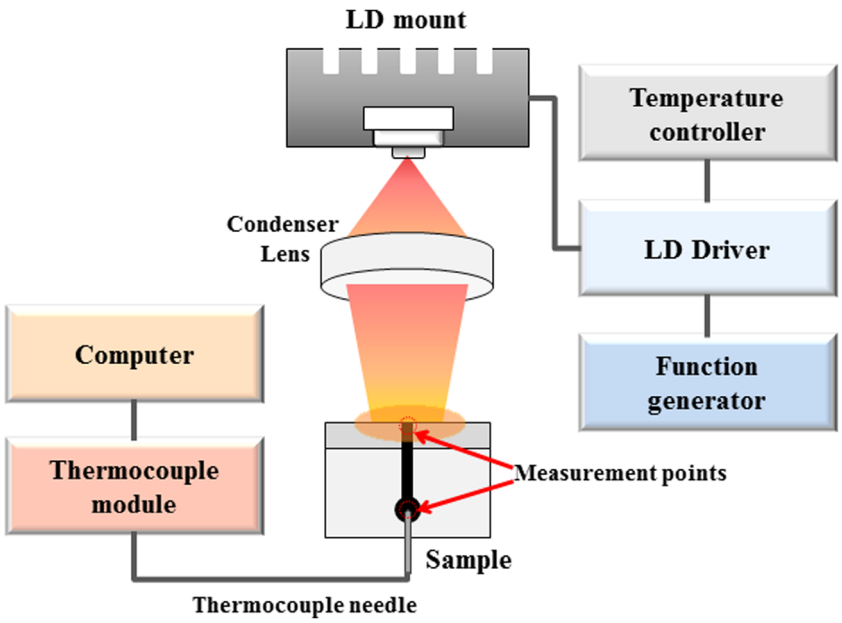

Fig. 2 Experimental setup for the validation of the developed heat diffusion model

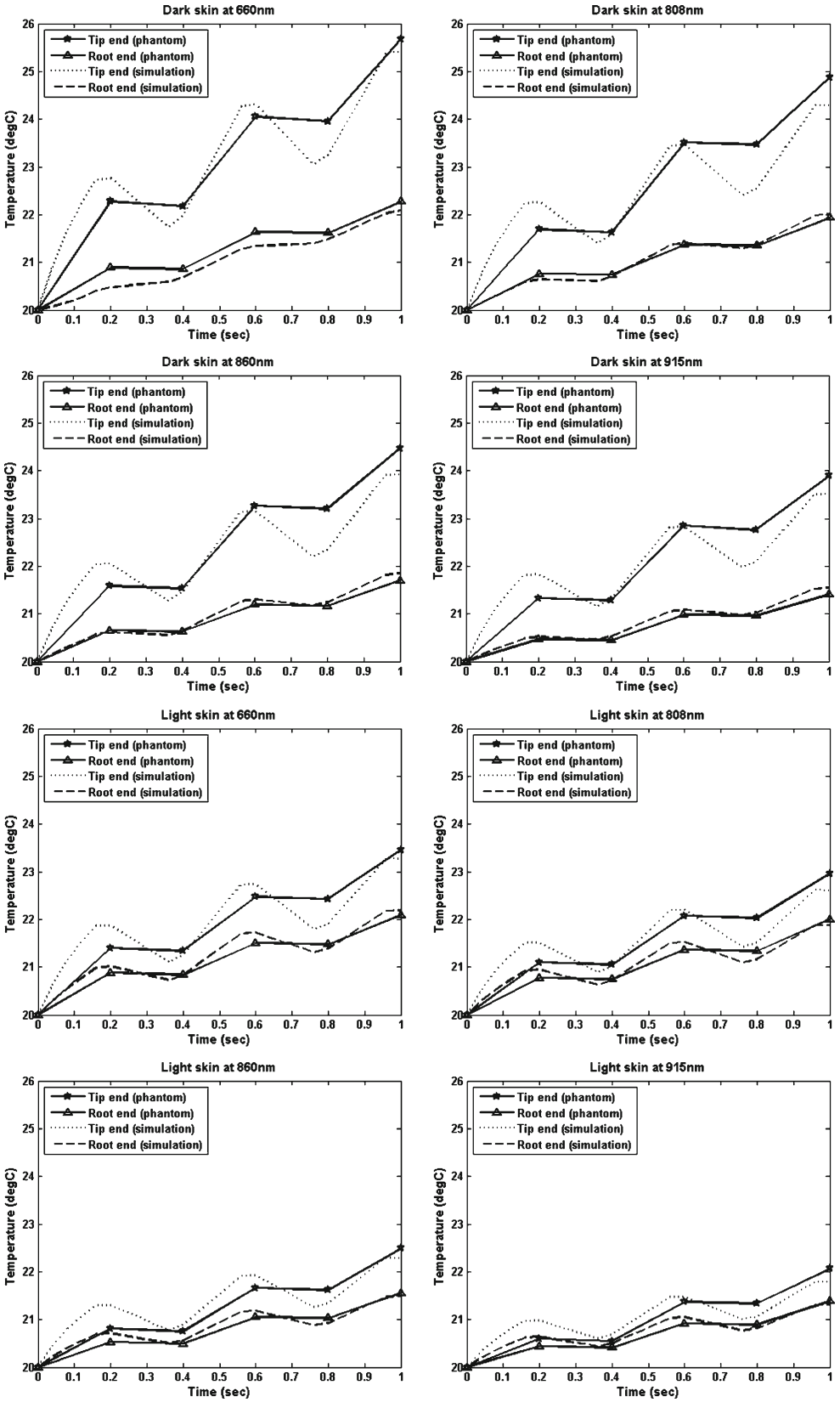

Fig. 3 Comparison of temperature changes between the experimental results and the numerical results at two designated points (hair tip and hair root tip)

Temperature distribution maps and changes over various wavelengths

Figure 4 shows the temperature changes from the numerical model subjected to three pulses of light in sequence where the fluence per pulse is 12 J/cm^2, which is in the range of available fluences for clinical purposes. We found that the calculated temperature distribution maps are in agreement with previous findings [21, 22]. Heat generation at the hair tip is significantly higher than in other portions, and this tendency always appears regardless of skin type or wavelength. We also observed that the temperature of the hair root corresponding to the hair follicle is higher than the hair shaft and dermis. The reasonable explanations for these results were provided by Sun et al. [21]. However, contrary to the previous 2D axisymmetric model, we could observe more details about the epidermal temperature distribution in our model and found that the melanin concentration in the epidermis can affect not only to the hair follicle but also to the boundary between the epidermis and the hair shaft. We can recognize that the higher epidermal melanin concentration in the dark skin model results in more intensive heat generation to the hair tip region when comparing Fig. 4a with c and Fig. 4b with d. The results also show that the heated epidermal surface elevates the overall temperature of the inner tissue structure such as the dermis and hair follicle through thermal conduction.

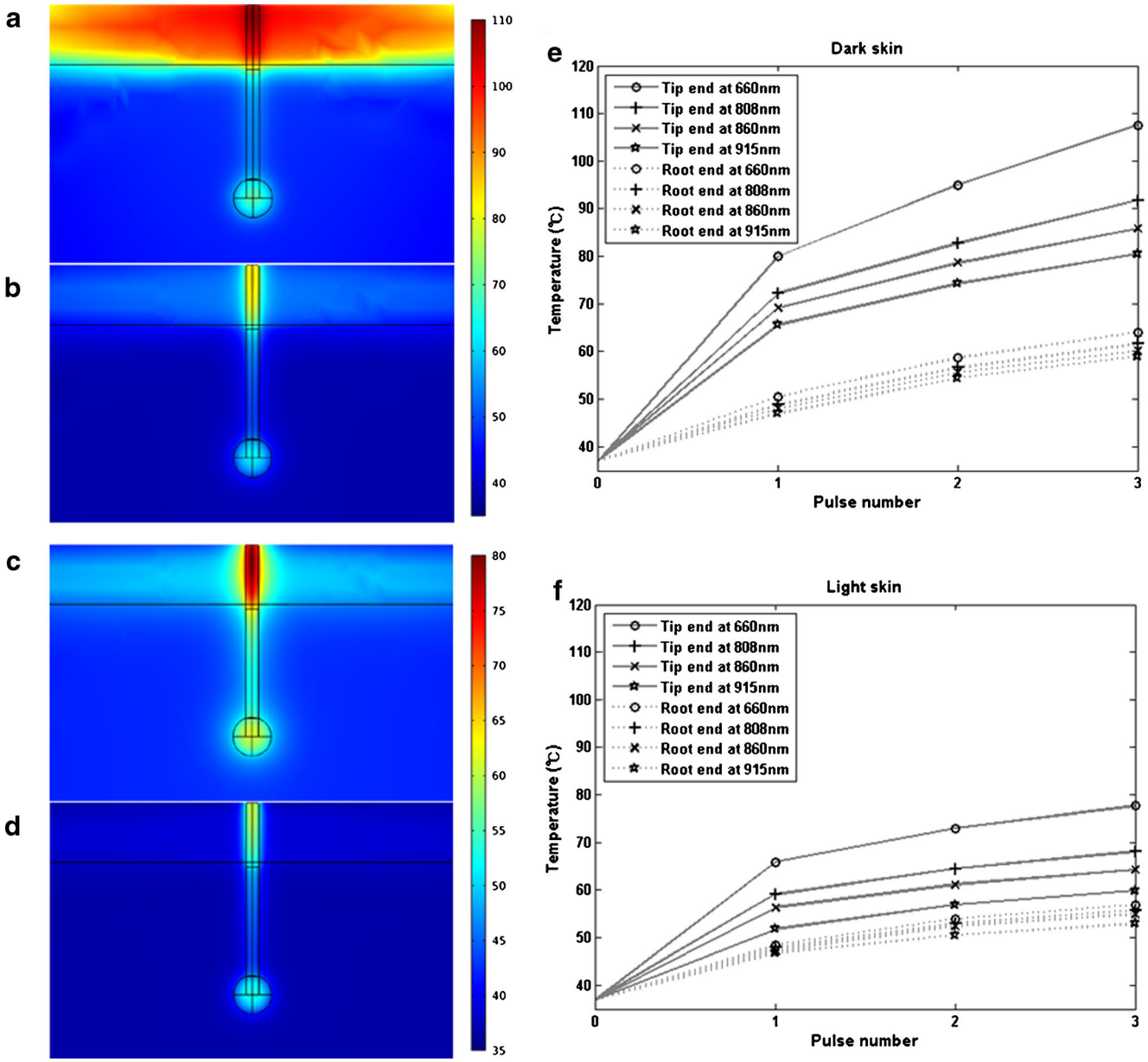

Fig. 4 **a**, **b**, **c** and **d** represent the temperature maps of the two antithetical skin types after the third light pulse applied at 660 and 915 nm, and **e** and **f** show the temperature increments at both hair tip and root according to the pulse sequence from all applied wavelengths

When looking at the temperature changes over four different wavelengths at two designated points (hair tip and root) in both the light and dark skin models, we found that the temperature of the hair tip is always greater than at the hair root. The results also show that the temperature gap between the tip and root of the hair decreases as the wavelength increases, and it increases as the fluence increases with the largest gap occurring for the dark skin model at 660 nm. One interesting thing is the temperature of the hair follicle. After the third pulse of light is applied, the average temperatures with standard deviation of the hair tip with both the dark and light skin are 91.4 °C (±11.7 °C) and 67.5 °C (±7.6 °C), respectively, whereas that of the hair root are 61.2 °C (±2.2 °C) and 55.2 °C (±1.7 °C), respectively. It means that the thermal effect on the hair follicle is not greatly dependent on the wavelength. We can also explain that the high root temperature in the dark skin model may be a result of thermal conduction through the heated epidermis. This tendency is also found in the experimental results in Fig. 3.

Examination of thermal confinement along the skin surface

Temperature distribution on the skin surface is one of the important aspects in laser hair removal in terms of thermal confinement. Figure 5 shows the temperature distribution along the skin surface after the third pulse light for both the dark and light skin models. Since a Gaussian-shaped laser beam was applied in the numerical model, the temperature falls steeply from the centre of the spot on the surface. Good thermal confinement is known to achieve minimal temperature increases around non-targeted regions; otherwise, adverse effects will more likely occur. As seen in Fig. 5, the light skin surface achieves good thermal confinement, and most heat occurs at the centre of the hair region regardless of the wavelength. This must be related to the relative lower melanin concentration of the epidermis. However, in the case of the dark skin model, thermal confinement is poorly achieved, particularly at 660 nm owing to the pigmented skin surface with higher melanin concentration, which may cause severe thermal damage to surrounding skin tissue. Comparatively, thermal confinement is achieved best at 915 nm.

From the results, we can expect that for the darker skin types, high-power lasers with wavelengths of 860 or 915 nm would induce thermal damage to the hair follicle comparable to that from a wavelength of 808 nm and achieve a better thermal confinement compared with other shorter wavelengths. In the case of the lighter skin types, owing to the almost perfect thermal confinement achieved, the shorter wavelengths (<808 nm) will result in better treatment

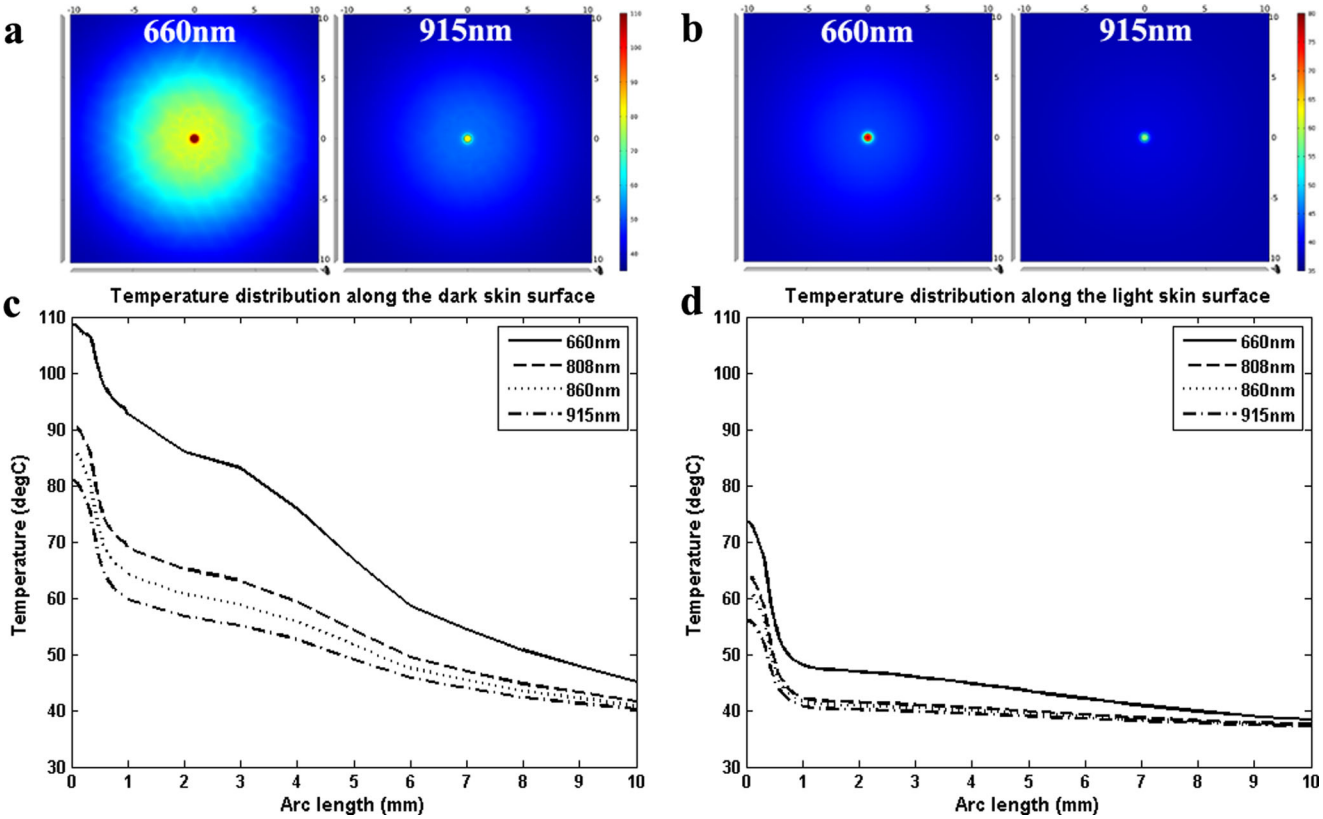

Fig. 5 **a** and **c** represent the temperature maps of skin surface (*top view*) after the third light pulse applied at 660 and 915 nm, and **b** and **d** show the temperature distribution along the skin surface after the third light pulse over four wavelengths for both the dark and light skin models

outcomes without concern for side effects. However, there are a few limitations that should be stressed in the present study. First, although the numerical HD simulation calculated the temperature distribution along the hair structure and skin tissue for various wavelengths, other important laser parameters in laser hair removal such as pulse width, fluence, and repetition rate have not been taken into account altogether in this study. This means that selecting an adequate wavelength for various skin types is only a part of establishing the optimal laser parameters, and these need to be considered in conjunction with the other parameters for clinical purposes. Secondly, we only examined two skin types with one hair colour in this study. As diverse as the skin colour, natural hair colour can be black, brown, blond, red, grey or white. This fact is intimately correlated with the treatment efficacy, because hair colour is dependent on the concentration of eumelanin and pheomelanin pigment in hair follicles [23], and this will be treated in our future research. Nevertheless, the proposed numerical model enables the calculation of the temperature distribution regarding the relationship between the wavelength and the skin types. In future research, various hair colours will be considered, and we will take other laser parameters into account in this proposed model.

Conclusion

In the present study, we developed a heat diffusion model considering skin types over various wavelengths. The optical properties of both light and dark skin were derived from the aforementioned formulas considering baseline skin absorption, melanin absorption and haemoglobin absorption. In order to validate the simulation model, an in vitro phantom experiment was conducted. Two-layered skin phantoms were prepared with hair structures, and the optical properties of each component were determined using an IAD method based on transmittance and reflectance measurements using integrating spheres. The experimental results were consequently well matched with the simulation results.

The simulation results demonstrate that in the case of the light skin model, thermal confinement is well achieved over various wavelengths, and treatment efficacy would be better using a shorter wavelength with minimal adverse effects compared with the dark skin model. However, in the case of the dark skin model, thermal confinement is poorly achieved using shorter wavelengths, which may result in significant unwanted side effects to the skin tissue. Therefore, it is expected that either 860 or 915 nm would be more suitable for darker skin types in terms of safety and treatment efficacy. Based on the results, we found that temperature distribution along the hair and skin surface is varied over the level of pigmentation on the skin. We believe that the developed numerical model will help to establish optimal laser parameters for different individuals during laser hair removal.

Acknowledgments This work was supported by research grants from the Catholic University of Daegu in 2013

References

1. Gold MH (2007) Lasers and light sources for the removal of unwanted hair. Clin Dermatol 25(5):443–453
2. Lavker RM, Miller S, Wilson C, Cotsarelis G, Wei ZG, Yang JS, Sun TT (1993) Hair follicle stem cells: their location, role in hair cycle, and involvement in skin tumor formation. J Investig Dermatol 101: 16S–26S
3. Anderson RR, Parrish JA (1983) Selective photothermolysis: precise microsurgery by selective absorption of pulsed radiation. Science 220:524–527
4. Fitzpatrick TB (1988) The validity and practicality of sun-reactive skin types I through VI. Arch Dermatol 124:869–871
5. Pathak MA, Fitzpatrick TB (1993) Preventive treatment of sunburn, dermatoheliosis, and skin cancer with sun protective agents. In: Fitzpatrick TB, Eisen AZ, Wolff K et al (eds) Dermatology in general medicine, 4th edn. McGrawHill, Inc, New York, pp 1689–1717
6. Wheeland RG (2007) Simulated consumer use of a battery-powered, hand-held, portable diode laser (810 nm) for hair removal: a safety, efficacy and ease-of-use study. Lasers Surg Med 39(6):476–493
7. Battle EF Jr, Hobbs LM (2004) Laser-assisted hair removal for darker skin types. Dermatol Ther 17(2):177–183
8. Battle EF, Anderson RR (2000) Study of very long-pulsed (100 ms) high-powered diode laser for hair reduction on all skin types. Coherent Medical, Santa Clara
9. Battle EF Jr, Soden CE Jr (2009) The use of lasers in darker skin types. Semin Cutan Med Surg 28:130–140
10. Ort RJ, Anderson RR (1999) Optical hair removal. Semin Cutan Med Surg 18:149–158
11. Breadon JY, Barnes CA (2007) Comparison of adverse events of laser and light-assisted hair removal systems in skin types IV-VI. J Drugs Dermatol 6(1):40–46
12. Jacques SL (2013) Optical properties of biological tissues: a review. Phys Med Biol 58(11):37–61
13. Alster TS, Bryan H, Williams CM (2001) Long-pulsed Nd:YAG laser-assisted hair removal in pigmented skin: a clinical and histological evaluation. Arch Dermatol 137(7):885–889
14. Campos VB, Dierickx CC, Farinelli WA, Lin TY, Manuskiatti W, Anderson RR (2000) Hair removal with an 800-nm pulsed diode laser. J Am Acad Dermatol 43(3):442–447
15. Gold MH, Foster A, Biron JA (2010) Low-energy intense pulsed light for hair removal at home. J Clin Aesthet Dermatol 3(2):48–53
16. Shen W, Zhang J, Yang F (2005) Modeling and numerical simulation of bioheat transfer and biomechanics in soft tissue. Math Comput Model 41(11–12):1251–1265
17. Eze R, Kumar S (2007) Modeling of fractional photothermolysis in dermatological applications. Proceedings of the COMSOL Conference, Boston
18. Jacques SL (1998) Skin optics. Webpage: http://omlc.ogi.edu/news/jan98/skinoptics.html
19. Lask G, Eckhouse S, Slatkine M, Waldman A, Kreindel M, Gottfried V (1999) The role of laser and intense light sources in photo-epilation: a comparative evaluation. J Cutan Laser Ther 1(1):3–13

20. Manns F, Milne PJ, Gonzalez-Cirre X, Denham DB, Parel JM, Robinson DS (1998) In situ temperature measurements with thermocouple probes during laser interstitial thermotherapy (LITT): quantification and correction of a measurement artifact. Lasers Surg Med 23(2):94–103
21. Sun F, Chaney A, Anderson R, Aguilar G (2009) Thermal modeling and experimental validation of human hair and skin heated by broadband light. Lasers Surg Med 41(2):161–169
22. Ataie-Fashtami L, Shirkavand A, Sarkar S, Alinaghizadeh M, Hejazi M, Fateh M, Esmaeeli Djavid G, Zand N, Mohammadreza H (2011) Simulation of heat distribution and thermal damage patterns of diode hair-removal lasers: an applicable method for optimizing treatment parameters. Photomed Laser Surg 29(7): 509–515
23. Lepselter J, Elman M (2004) Biological and clinical aspects in laser hair removal. J Dermatol Treat 15(2):72–83